Kinetics and Mechanism of the Reaction of $^{\bullet}NH_2$ with O_2 in Aqueous Solutions

B. Laszlo, Z. B. Alfassi, P. Neta, and R. E. Huie*

Physical and Chemical Properties Division, National Institute of Standards and Technology, Gaithersburg, Maryland 20899

Received: March 17, 1998; In Final Form: June 11, 1998

The reaction of NH_3 with $^{\bullet}OH$ or $SO_4^{\bullet-}$ radicals produces the aminyl radical, $^{\bullet}NH_2$. Pulse radiolysis and laser flash photolysis techniques were utilized to study the formation of this radical, its absorption spectrum, its reaction with O_2, and the mechanism of formation of subsequent intermediates and the main final product, peroxynitrite. The rates of formation of $^{\bullet}NH_2$ and its absorption spectrum are in agreement with previous reports. The reaction of $^{\bullet}NH_2$ with O_2, however, was observed to take place much more rapidly than reported before and to involve an equilibrium of these reactants with the aminylperoxyl radical, $NH_2O_2^{\bullet}$. The equilibrium is shifted toward completion of the reaction via catalyzed decomposition of this peroxyl radical, and this decomposition affects the observed rate of reaction of $^{\bullet}NH_2$ with O_2. The peroxyl radical deprotonates and isomerizes and finally forms NO. In the presence of $O_2^{\bullet-}$, NO is converted rapidly to peroxynitrite, ONO_2^-. This product, which is stable at alkaline pH, was confirmed by γ-radiolysis of aerated ammonia solutions.

Introduction

The kinetics and mechanism of the oxidation of ammonia are of interest both in atmospheric chemistry and in water-cooled nuclear reactors. In both cases, the oxidation of ammonia can be initiated by the hydroxyl radical,

$$^{\bullet}OH + NH_3 \rightarrow H_2O + {}^{\bullet}NH_2 \qquad (1)$$

with a rate constant of 9.5×10^7 L mol^{-1} s^{-1} in the gas phase[1] and 9.7×10^7 L mol^{-1} s^{-1} in the aqueous phase.[2] The product aminyl radical, $^{\bullet}NH_2$, reacts extremely slowly, if at all, with molecular oxygen in the gas phase, with a reported upper limit of 0.1 L mol^{-1} s^{-1} for the production of nitrogen oxides.[3] In the aqueous phase, however, the reaction appears to be fast, although there is poor agreement on the absolute magnitude of the rate constant. The kinetics of this reaction have been measured by pulse radiolysis by following either the decay of the very weak absorption of $^{\bullet}NH_2$ at 530 nm or the formation of a long-lived reaction product at 300 nm. Rate constants of 3×10^8 L mol^{-1} s^{-1} [4] and 1.2×10^8 L mol^{-1} s^{-1} [5] were derived from the absorption decay, but rate constants of $\sim 1 \times 10^7$ L mol^{-1} s^{-1} [6] and 3.4×10^7 L mol^{-1} s^{-1} [7] were obtained in the studies in which product formation was followed. This product, absorbing at 300 nm, was suggested to be NH_2O_2, on the basis of a similar absorption in liquid ammonia.[8] This assignment, however, was rejected by more recent experiments which showed that the 300 nm band is not observed in the pulse radiolysis of ammonia solutions in the presence of persulfate as an electron scavenger.[5] These authors suggested that the 300 nm band may be ascribed to $NH_2O_2^-$ formed by the following reactions

$$^{\bullet}NH_2 + O_2 \rightarrow NH_2O_2^{\bullet} \qquad (2)$$

$$e_{aq}^- + O_2 \rightarrow O_2^{\bullet-} \qquad (3)$$

$$O_2^{\bullet-} + NH_2O_2^{\bullet} \rightarrow O_2 + NH_2O_2^- \qquad (4)$$

and they derived a rate constant of $k_4 = 6.6 \times 10^9$ L mol^{-1} s^{-1}. More detailed examination[9] of the 300 nm absorption indicated that the decay rate decreases at high pH and that the absorption has a peak at 290 nm at short times, but that the peak shifts to 305 nm at long times. The product responsible for the 305 nm absorption was found to be long-lived, with a half-life greater than 10 min.

Nitrite has been reported to be the main final radiolysis product of aqueous ammonia solutions.[10] In experiments involving the continuous X-ray irradiation of air-saturated aqueous NH_3 solutions at pH 11.4, the formation of a product absorbing at 305 nm also was observed. This product slowly changed to a more stable product absorbing at 210 nm, which was taken to be due to NO_2^- ions.[9] The 305 nm absorption was not detected at pH < 10, and its stability increased with pH; at pH > 12 the half-life of this product was several hours.[9] The authors suggested that this product is peroxynitrite, O=N−O−O$^-$, which is rather stable at high pH. This is in agreement with earlier findings[11] that γ-irradiation of oxygen-containing aqueous ammonia solutions leads to production of peroxynitrite. The yield was 0.66 μmol J^{-1} for $[NH_3] = 6-15$ mol L^{-1} [11] but only 0.10, 0.22, and 0.39 at $[NH_3] = 1 \times 10^{-3}$, 1×10^{-2}, and 1.5×10^{-1} mol L^{-1}, respectively.[9] The mechanism suggested by Mikhailova et al. for formation of peroxynitrite involved a reaction of $NH_2O_2^{\bullet}$ with $O_2^{\bullet-}$.

$$NH_2O_2^{\bullet} + O_2^{\bullet-} \rightarrow H_2O + O{=}N{-}O{-}O^- \qquad (5)$$

Reaction 5 is rather complex, as it requires several bonds to be broken and formed simultaneously. Schönherr et al.[11] suggested two different stepwise mechanisms for the last reaction, either

$$NH_2O_2^{\bullet} + O_2^{\bullet-} \rightarrow HN^{\bullet}OO^{\bullet} + HO_2^- \rightarrow ONOO^- + H_2O \qquad (6)$$

or

$$NH_2O_2^{\bullet} + O_2^{\bullet-} \rightarrow NH_2O_2^- + O_2 \qquad (7)$$

$$NH_2O_2^- \rightarrow NO^- + H_2O \qquad (8)$$

$$NO^- + O_2 \rightarrow ONOO^- \qquad (9)$$

An alternate explanation for the formation of peroxynitrite has

10.1021/jp981529+ This article not subject to U.S. Copyright. Published 1998 by the American Chemical Society
Published on Web 07/15/1998

been proposed involving the decomposition of NH_2O_2 into NO and H_2O, possibly through the intermediate formation of $HONO^-$.[12] Peroxynitrite is then produced by

$$NO + O_2^{\bullet-} \rightarrow OONO^- \qquad (10)$$

for which $k_{10} = 6.7 \times 10^9$ L mol^{-1} s^{-1}.[13] All of these mechanisms, however, predict the yield of $ONOO^-$ to be no more than that of OH radicals (0.28 μmol J^{-1}) and thus are not in agreement with the experimental *G* values. Because of these inconsistencies in the *G* values for peroxynitrite formation and to clarify the mechanism of the aqueous-phase oxidation of ammonia, we have undertaken an investigation of this system utilizing continuous radiolysis, pulse radiolysis, and laser flash photolysis.

Experimental Section[14]

Laser flash photolysis experiments employed an apparatus that was recently used in gas-phase studies.[15,16] The beam from a Questek model 2320 excimer laser, operated at 248 nm, was expanded by a cylindrical lens to fill a portion of a 5 cm diameter, 10 cm long cylindrical quartz cell through a 2 × 10 cm flat Suprasil window. The analysis light from a 75 W xenon arc lamp was rendered nearly parallel by using a condenser and two long focal-length lenses and passed four times through the reaction cell, which was located between two mirrors. After traversing the cell, the light was deflected by a prism and then divided by a beam splitter, with each half of the analysis beam focused on the entrance slit of a monochromator. A fast shutter was located between the xenon lamp and the reaction cell to reduce the extent of photolysis by the analyzing light. Cutoff filters also were employed before the reaction cell, when appropriate.

Electronic signals from the photomultipliers were fed into a two-channel, multi-timebase waveform digitizer through differential comparators. In the absence of a transient absorber, the voltage from the photomultiplier (typically about 100 mV) was balanced by a reference voltage. Following laser flash photolysis, the transient signal was read by the digitizer as the difference between the reference voltage and the actual signal. After each flash, the data from the transient analyzer were read by a computer and averaged into memory. Every 50 flashes, I_0 (the voltage from the photomultiplier before the flash) was read using a digital voltmeter. This I_0 value was then used to convert the transient voltage signal into a transient absorption. With this arrangement, we found that we could safely resolve an absorbance change of 4×10^{-4}. The cell was operated in a continuous flow mode with a peristaltic pump located after the reaction cell. Total flow rates of 20−25 mL min^{-1} were used to prevent the accumulation of reaction products. The laser was run at a repetition rate of 0.3−1.0 Hz. All experiments were performed at ambient temperature (293 ± 2 K).

Pulse radiolysis studies were carried out with the same apparatus used in our previous study of the reaction of NH_2 with SO_3^{2-}.[17] Solutions were irradiated by 50 ns pulses of 2 MeV electrons supplied by a Febetron 705 accelerator. The dose per pulse was usually about 10−30 Gy, determined by KSCN dosimetry. The single-pass optical detection system consisted of a 300 W xenon lamp, separated from the cell by a shutter, and a monochromator and photomultiplier located in a separate room from the irradiation zone, with appropriate optics to focus the light through the front of the cell, collect the transmitted light, and focus it again onto the monochromator slit. Before the pulse, the optical signal was measured by a sample-and-hold circuit and the change in absorbance after the pulse monitored with a differential amplifier. The kinetic traces were digitized by a transient amplifier and rate constants derived by least-squares analysis.

γ-Radiolysis studies were carried out by using a Gammacell 220 ^{60}Co source. Ammonia solutions were placed in 1 cm Suprasil quartz cuvettes and saturated with either N_2O or O_2. The cells were irradiated at a dose rate of 56 Gy min^{-1} for varying periods, and the production of stable products was determined by measuring the UV−visible absorption spectrum.

Results

The formation and reactions of $^{\bullet}NH_2$ radicals were studied by radiolytic and photolytic methods. In the radiolysis experiments, $^{\bullet}NH_2$ radicals were produced by the reaction of $^{\bullet}OH$ radicals with NH_3, and in the photolysis experiments, they were produced by the reaction of $SO_4^{\bullet-}$ radicals with NH_3. The NH_3 solutions were prepared either by diluting concentrated ammonium hydroxide solutions with water or by preparing solutions of $(NH_4)_2SO_4$ and adjusting the pH to the alkaline region. The objective of this study was to understand better the mechanism and rate of the reaction of $^{\bullet}NH_2$ with O_2 in aqueous solution. We describe first laser flash photolysis studies of the reaction, then pulse radiolysis studies, and, finally, the γ-radiolytic conversion of NH_3 to peroxynitrite.

Laser Flash Photolysis Studies. The $^{\bullet}NH_2$ radical was produced in these experiments by the 248 nm photolysis of persulfate ions in the presence of ammonia, according to the reactions

$$S_2O_8^{2-} + h\nu \rightarrow 2SO_4^{\bullet-} \qquad (11)$$

$$SO_4^{\bullet-} + NH_3 \rightarrow SO_4^{2-} + H^+ + {}^{\bullet}NH_2 \qquad (12)$$

In these studies, we determined the rate constant for reaction 12, the absorption spectrum of the $^{\bullet}NH_2$ radical and its self-reaction rate constant, and, finally, the kinetics and mechanism of its reaction with O_2.

Rate Constant for the Reaction of $SO_4^{\bullet-}$ with NH_3. The $SO_4^{\bullet-}$ radicals were generated by laser photolysis of aqueous solutions containing 1−2 mmol L^{-1} $Na_2S_2O_8$ or $(NH_4)_2S_2O_8$. In the latter case no additional ammonia source was used while in the former case, 1.6−14 mmol L^{-1} $(NH_4)_2SO_4$ was added. The NH_3 concentration range was set by adjusting the pH by the addition of 1−3 mL of saturated NaOH solution. The ammonia concentration can be calculated from the concentration of the ammonium salt dissolved, *C*, the pH value, and the dissociation constant of ammonium hydroxide, [18] $K_b = 1.79 \times 10^{-5}$, according to

$$[NH_3] = \frac{C[OH^-]}{K_b} \Big/ \left(1 + \frac{[OH^-]}{K_b}\right)$$

With the pH between 8.4 and 10.8, the NH_3 concentration ranged from 0.36 to 12 mmol L^{-1}. The absorption of the $SO_4^{\bullet-}$ radical was monitored at 450 and 530 nm. The decay followed clean first-order kinetics, where the dominant loss of $SO_4^{\bullet-}$ was via its reaction with NH_3 (k_{12}), but with a few percent contribution from its reaction with OH^-, $k = 1.4 \times 10^7$ L mol^{-1} s^{-1} ,[19] and with water, $k = 440$ s^{-1}.[20] The $SO_4^{\bullet-}$ decay rate constants, corrected for these reactions, are linearly dependent on $[NH_3]$ (Figure 1), giving $k_{12} = (1.1 \pm 0.1) \times 10^8$ L mol^{-1} s^{-1}, where the uncertainty limit is twice the standard deviation of the linear least-squares fit. In these experiments the highest

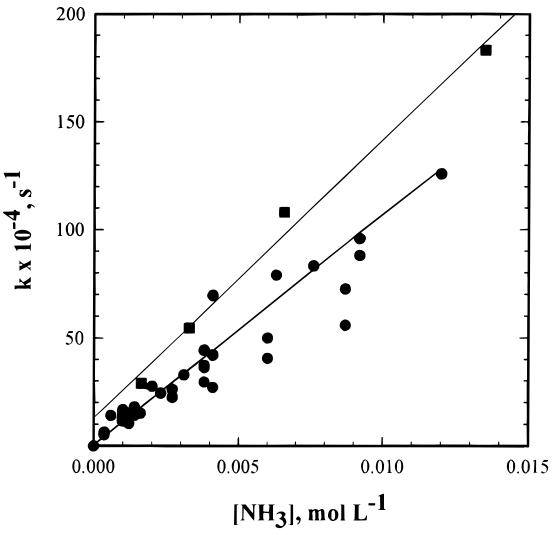

Figure 1. Rate constant for the decay of $SO_4^{\bullet-}$ as a function of NH_3 concentration. The $SO_4^{\bullet-}$ was produced by laser flash photolysis (circles) or by pulse radiolysis (squares).

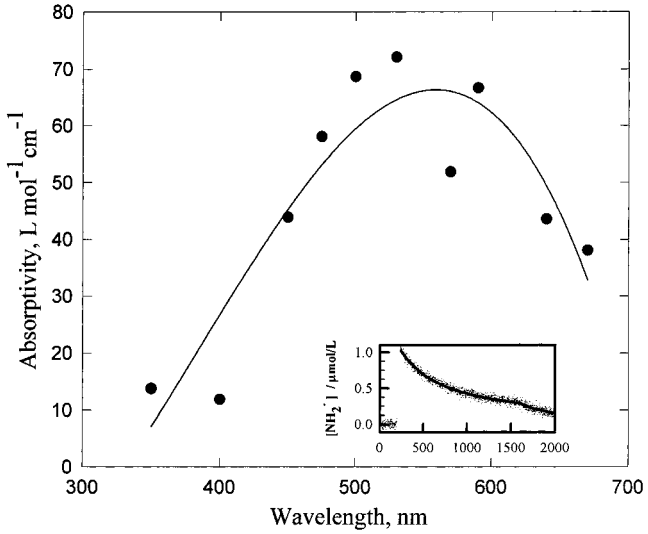

Figure 2. Spectrum of the $^{\bullet}NH_2$ radical, obtained by laser flash photolysis. Inset: decay of absorption due to $^{\bullet}NH_2$ at 520 nm with no O_2 present. The time scale is 0.5 μs per channel up to channel 1600 and 2 μs beyond.

uncertainty was that of the pH determination, which was estimated to be better than ±0.1 pH units.

Absorption Spectrum of the $^{\bullet}NH_2$ Radical. The molar absorptivity of the $^{\bullet}NH_2$ radical was determined relative to the 450 nm $SO_4^{\bullet-}$ absorbance. In deoxygenated 0.04−0.1 mol L^{-1} NH_3 solutions, the formation of $^{\bullet}NH_2$ (i.e., the SO_4^{-} decay) and its removal via self-reaction are well separated in time. The absorbance could be read directly from the experimental curves, with no extrapolation necessary. Taking $\epsilon_{450} = 1630$ L mol^{-1} cm^{-1} for the $SO_4^{\bullet-}$ radical from Buxton et al.,[21] which is in agreement with earlier determinations,[22,23] molar absorptivities of $\epsilon_{530} = 81 \pm 21$ and $\epsilon_{450} = 52 \pm 12$ L mol^{-1} cm^{-1} were determined (uncertainties are 2σ from 19 experiments). At these two wavelengths, the molar absorptivities were independent of the spectral bandwidth (0.3, 0.7, and 1 nm), confirming that the spectrum is not composed of several sharp peaks as in the gas phase.[24] Less detailed experiments between 350 and 670 nm (Figure 2) resulted in the same broad, featureless weak absorption band as described in the literature.[4] The contrast between this spectrum and that observed in the gas phase indicates that $^{\bullet}NH_2$ is highly solvated in water. This may be another reason for the very large difference in the reactivity of $^{\bullet}NH_2$ with O_2 in the two phases. It should be pointed out that other radicals, for example $NO_3^{\bullet}$, retain a structured spectrum from the gas phase to aqueous solutions.[25]

The value for ϵ_{530} is very close to values reported previously. Pagsberg reported $\epsilon_{530} = 81$ L mol^{-1} cm^{-1}. [4] Ershov et al. argued that the calculation leading to this value neglected the decay of $^{\bullet}NH_2$ during the 1 μs pulse.[7] They recalculated it to be close to their experimental value of 92 L mol^{-1} cm^{-1}, which was calculated by taking into account the decay of $^{\bullet}NH_2$ during their 2.3 μs pulse. Men'kin et al.[26] also used a 2.3 μs pulse and derived ϵ_{530} of 84 L mol^{-1} cm^{-1}. Since we are using a much shorter pulse and a direct comparison with ϵ for $SO_4^{\bullet-}$, our result should be the most reliable.

Self-Reaction of the $^{\bullet}NH_2$ Radical. In the absence of oxygen, $^{\bullet}NH_2$ radicals combine to form hydrazine. The second-order rate constant for this reaction was determined by following the absorbance decay at 530 and 450 nm. A typical experimental curve is shown as an inset in Figure 2 along with the calculated decay curve. Six experiments resulted in an average of $k = (2.2 \pm 0.2) \times 10^9$ L mol^{-1} s^{-1} where the uncertainty is twice the standard deviation of the average. This value is in excellent agreement with the previous determination.[4]

Reaction of $^{\bullet}NH_2$ Radicals with O_2. The reaction of the aminyl radical with molecular oxygen was investigated in concentrated NH_3 solutions, ∼1.5 mol L^{-1}, and, primarily, in solutions containing 0.06−0.12 mol L^{-1} NH_3. The experiments in concentrated ammonia were carried out by mixing N_2-saturated ammonia solutions with air-saturated water, both containing 1 mmol L^{-1} sodium persulfate. The results from these studies were erratic, and a plot of the first-order decay rate constants against the oxygen concentration resulted in a quite high intercept. The slope of this plot indicated a second-order rate constant of about 9×10^8 L mol^{-1} s^{-1}.

For the other measurements on the reaction of $^{\bullet}NH_2$ with O_2, aqueous solutions containing 1 mmol L^{-1} $Na_2S_2O_8$ and 0.03−0.06 mol L^{-1} $(NH_4)_2SO_4$ were first bubbled thoroughly with a known mixture of O_2/N_2, and then the pH was adjusted to 9.3−9.6 with saturated NaOH and the gas inlet frit lifted above the liquid level to minimize the escape of NH_3, although the results are not critically dependent on $[NH_3]$ provided that it remained high enough. Under these conditions, reaction 12 was complete within 1−2 μs after the laser flash, and the strong absorbance from $SO_4^{\bullet-}$ did not interfere with the measurement of the $^{\bullet}NH_2$ radicals, which were monitored at 530 nm. Upon addition of O_2, the decay rate for $^{\bullet}NH_2$ increased significantly. This absorption decay did not follow clean first-order kinetics, even though the oxygen concentration was in great excess over that of the aminyl radical. Logarithmic transforms of the curves showed a steep linear decay at initial times, and then the decay slowed. This pattern may be due either to secondary formation of other absorbing products or to the reaction of $^{\bullet}NH_2$ radicals with O_2 being a reversible process. The initial slopes of the logarithmic transform can be regarded as lower limits to the first-order rate constants for the $^{\bullet}NH_2 + O_2$ reaction. These values, plotted against $[O_2]$ (Figure 3), show a linear dependence which results in a second-order rate constant of $(3.0 \pm 0.2) \times 10^8$ L mol^{-1} s^{-1}, the same value as reported by Pagsberg.[4]

Figure 4(top) shows the absorptions measured at 280 and 320 nm after the flash photolysis of aqueous solutions of persulfate and ammonia in the presence of molecular oxygen, after subtraction of the contribution to the absorption due to $SO_4^{\bullet-}$. The traces reveal two new absorption features. The first, which

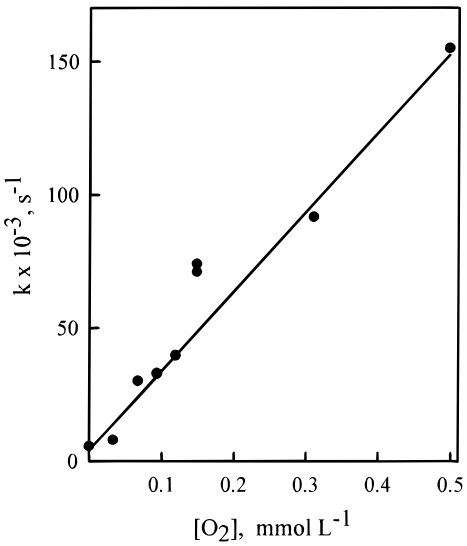

Figure 3. Initial rate of decay of $^{\bullet}NH_2$ as a function of O_2.

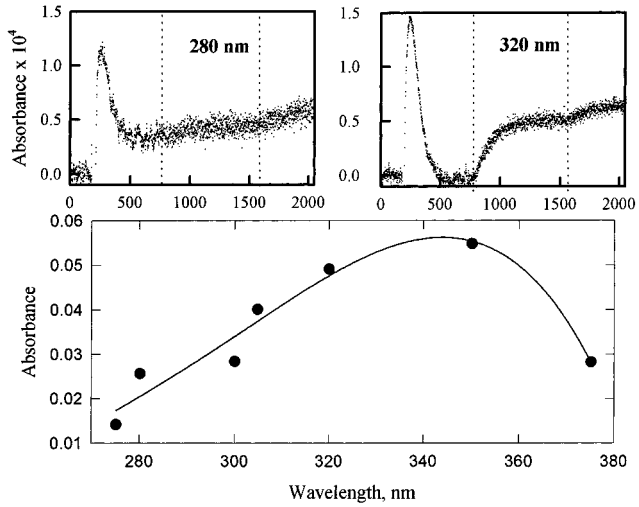

Figure 4. Spectrum of the $NH_2O_2^{\bullet}$ radical. Inset: experimental traces at 280 and 320 nm, resulting from the reaction of $^{\bullet}NH_2$ with O_2. The elapsed time up to the first vertical dashed line is 16 μs, to the second vertical dashed line, 400 μs, and to the end, 31 ms. Absorption due to $SO_4^{\bullet-}$ has been subtracted, and the spectrum is derived from the extrapolated absorption maximum at short time.

rapidly forms and decays, is centered about 340 nm. The spectrum of this short-lived absorption, also shown in Figure 4, is similar to a spectrum observed after the photolysis of KO_3 in liquid NH_3 which was ascribed to the aminylperoxyl radical, NH_2O_2.[8] This undergoes a first-order decay; the decay rate increased linearly with oxygen concentration up to about 4×10^{-4} mol L^{-1} but appeared to plateau at a concentration of 1.3×10^{-5} mol L^{-1} (Figure 5). At 320 nm, the absorption decays to zero before increasing. At 280 nm, there is some residual absorption at intermediate times, which we ascribe to a small amount of $^{\bullet}O_2^-$ formed in the flash (see below).

After the decay of this short-lived species, identified as NH_2O_2, a long-lived absorption builds up at much longer times. (Note the change in time scales in Figure 4.) This long-lived absorption is centered around 305 nm, and its spectrum (not shown) appears identical to that observed for peroxynitrite.[13] An examination of the traces in Figure 4 also reveals that the long-lived absorption arises from a species formed in a secondary process and is not due to a direct product of the reaction of $^{\bullet}NH_2$ with O_2. Assuming this long-lived species is peroxynitrite, $^-$OONO, the yield is less than 1%, based on the

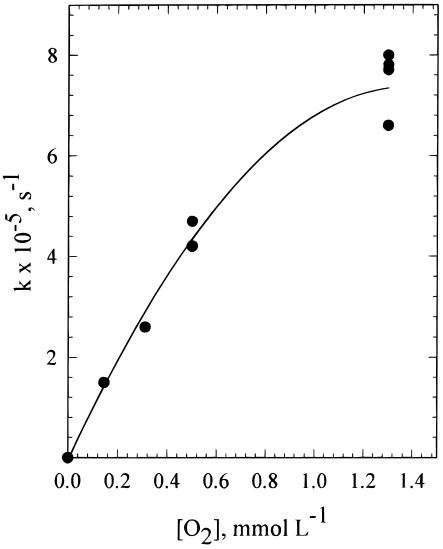

Figure 5. Decay rate of the $NH_2O_2^{\bullet}$ radical plotted against O_2 concentration.

known absorption coefficient for this species of 1670 L mol^{-1} cm^{-1}.[27] This low yield, along with the disconnect between the decay of NH_2O_2 and the formation of $^-$OONO, supports a mechanism in which NO is formed from NH_2O_2 and reacts with the small amount of $^{\bullet}O_2^-$ formed from the flash.

Pulse Radiolysis Studies. *Rate Constant for the Reaction of $SO_4^{\bullet-}$ with NH_3.* The rate constant measured in the flash photolysis studies above is considerably higher than that measured previously by pulse radiolysis.[6] Therefore, we reexamined this reaction by irradiating, with an electron pulse, air-saturated aqueous solutions containing varying concentrations of $(NH_4)_2S_2O_8$ at a constant pH of 9.6. In these solutions the e_{aq}^- reacts with the persulfate ion to form the $SO_4^{\bullet-}$ radical, and the $^{\bullet}OH$ radical is scavenged by the NH_3. The observed first-order rate constant for the decay of the 450 nm absorption was found to be linear with [NH_3] (Figure 1), and the second-order rate constant was calculated to be $k_{12} = (1.3 \pm 0.2) \times 10^8$ L mol^{-1} s^{-1}, suggesting that the earlier reported value, which is an order of magnitude lower, is probably in error.

Reaction of $^{\bullet}NH_2$ Radicals with O_2. The $^{\bullet}NH_2$ radical absorbs at 530 nm, but the molar absorptivity is only 81 L mol^{-1} cm^{-1} (see above). This low absorptivity prevents us from measuring the rate constant for reaction of $^{\bullet}NH_2$ with O_2 by directly following the decay of the $^{\bullet}NH_2$ absorbance with our pulse radiolysis apparatus (which does not permit significant signal averaging). Therefore, we resorted to competition kinetics methods. We chose ZnTSPP (zinc tetrakis-4-sulfonatophenylporphyrin) as the reference compound because it can be oxidized to form a strongly absorbing radical cation ($\lambda_{max} \sim$ 680 nm, $\epsilon_{max} \sim 10^4$ L mol^{-1} cm^{-1}).[28] The $^{\bullet}NH_2$ radical was produced by the pulse radiolysis of 0.8−1.5 mol L^{-1} NH_3 solutions containing both N_2O and O_2. Solutions were prepared in two ways: by saturating a stock solution with a mixture of N_2O and O_2, made by flowing the separate gases through a gas mixer with two flowmeters, or by mixing various proportions of a 1.5 mol L^{-1} NH_3 solution saturated with N_2O with an air-saturated solution that does not contain NH_3. Both solutions contained the same concentration of ZnTSPP. In the former method, we assumed that the solubility of O_2 in 1.5 mol L^{-1} NH_3 solutions is similar to that in pure water. The latter method was used to avoid this uncertainty.

Although ZnTSPP reacts with $^{\bullet}OH$ radicals nearly 2 orders of magnitude more rapidly than does NH_3, its concentration was

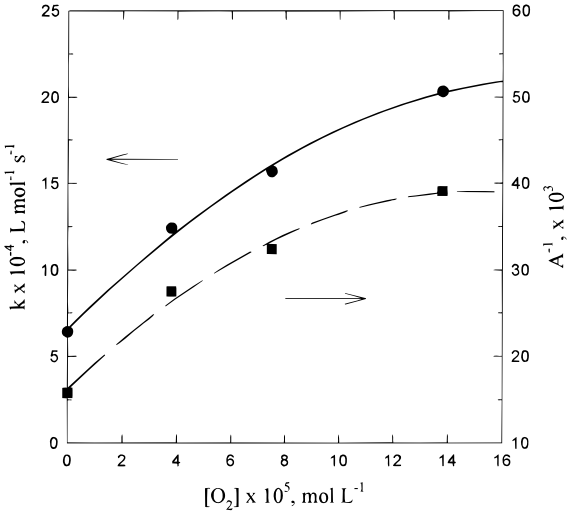

Figure 6. Competition kinetics to determine the rate constant for reaction of $^{\bullet}NH_2$ with O_2 using ZnTSPP as the reference compound. The absorbance (*A*) and the rate of formation of the radical cation (*k*) of this compound were monitored at 680 nm.

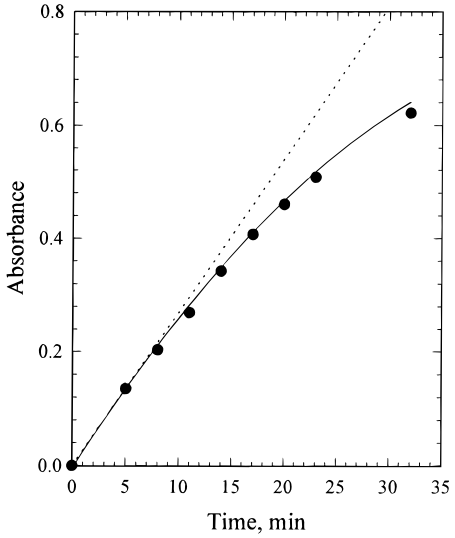

Figure 7. Formation of peroxynitrite, as measured by its absorbance at 302 nm, following γ-radiolysis of O_2-saturated aqueous solutions containing 1.5 mol L^{-1} NH_3 at pH 11.8. Dotted line represents full yield of peroxynitrite.

4 orders of magnitude lower. Therefore, the $^{\bullet}OH$ radicals produced by the radiolysis react predominantly with the NH_3. The $^{\bullet}NH_2$ radical was found to react with ZnTSPP to form the π-radical cation, with an absorption peak at 680 nm. Addition of O_2 to the solution leads to an increase in the observed first-order rate constant for the formation of the 680 nm absorption and a decrease in the final absorbance. The observed rate constant as a function of $[O_2]$, at constant [ZnTSPP], should follow the equation $k_{obs} = k_0 + k_2[O_2]$, where k_2 is the rate constant for the reaction of $^{\bullet}NH_2$ with O_2. The experimental results obtained (Figure 6) show significant curvature in the plot of k_{obs} vs $[O_2]$. Although part of the curvature may be due to experimental uncertainties, sufficient experiments were carried out to indicate that the curvature is real. A slightly higher curvature was observed with the mixed solutions method, possibly due to changes in the NH_3 concentration. The rate constant for the reaction of $^{\bullet}NH_2$ with O_2, as derived from the competition with ZnTSPP, can be estimated to be between $\sim 2 \times 10^9$ L mol^{-1} s^{-1} from the points for low $[O_2]$ to $\sim 1 \times 10^9$ L mol^{-1} s^{-1} from the points for high $[O_2]$.

We have attempted also to measure the rate of formation of the product absorbing at 300 nm by pulse radiolysis in the absence of ZnTSPP. Solutions containing 0.01 or 0.1 mol L^{-1} $(NH_4)_2SO_4$ in the pH range 9.0−9.6, which were either air-saturated or saturated with a 4/1 mixture of N_2O/O_2, were employed. We found very rapid formation of the absorption at 300 nm, with $k_{obs} \sim 2 \times 10^6$ s^{-1}. Even in the air-saturated solutions, where the initial $^{\bullet}O_2^-$ concentration would be equal to the $^{\bullet}NH_2$ concentration and the rate of formation of the long-lived species is faster, we were able to observe the absorption due to the short-lived intermediate. The decay of this species appeared to be more rapid at the higher ammonia concentration, which could reflect catalysis either by NH_3 or by OH^-. In the N_2O/O_2-saturated solutions, much less of the long-lived absorption is observed. This is due to the scavenging of the e_{aq}^- by the N_2O, which prevents the formation of $^{\bullet}O_2^-$. This further underlines the role of this radical in the formation of the long-lived absorbance.

γ-Radiolysis of Ammonia Solutions and Formation of Peroxynitrite. The observation of the formation of a small amount of ^-OONO in the flash photolysis experiments prompted us to study the reaction under conditions where the initial $^{\bullet}O_2^-$ yield would be the same as the $^{\bullet}NH_2$ yield. This was done by γ-irradiation of ammonia solutions. Radiolysis results in the formation of equal amounts of $^{\bullet}OH$ and e_{aq}^-. The $^{\bullet}OH$ reacts with NH_3 to yield $^{\bullet}NH_2$. In the presence of N_2O, the e_{aq}^- is converted to additional $^{\bullet}OH$, whereas in an O_2-saturated solution, $^{\bullet}O_2^-$ is generated. γ-Irradiation of N_2O-saturated aqueous ammonia (1.5 mol L^{-1}) solutions at pH 11.8 led to formation of products absorbing below 300 nm, probably N_2H_4 formed by combination of two $^{\bullet}NH_2$ radicals. Irradiation of O_2-saturated solutions of ammonia led to formation of a long-lived product with a maximum absorption at 305 nm, identical to the known spectrum of peroxynitrite.[27] The concentration of this product increased with the radiation dose (Figure 7) but not in a completely linear manner. The deviation from linearity at higher doses cannot be ascribed to thermal decomposition of the peroxynitrite product because this product was quite stable under these conditions. Also, only 20% of the oxygen is estimated to be consumed at this stage, so the curvature is not due to depletion of oxygen. Therefore, the curvature in Figure 7 is ascribed to destruction of peroxynitrite by reaction with radiation-produced radicals. The main reaction is that of peroxynitrite with e_{aq}^-, which leads to decomposition of this product and, in addition, competes with the production of $O_2^{\bullet -}$. To test this, we have modeled the system. First, we assumed that the lowest data point represented a full yield of peroxynitrite. By taking the reported molar absorptivity of $ONOO^-$ of 1670 L mol^{-1} cm^{-1},[27] we calculate a radiation yield of 0.28 μmol J^{-1}, which is consistent with the known yield of hydroxyl radicals and solvated electrons from the irradiation of water. Including this production rate in the model, all of the known reactions of $^{\bullet}OH$ and e_{aq}^- with each other and with the other constituents of the system, the expected production and reactions of $H^{\bullet}$ and H_2O_2, and the unimolecular decay rate constant for $ONOO^-$ at this pH ($k = 5 \times 10^{-6}$ s^{-1}),[29] we calculated predicted curves for the formation of $OONO^-$. With a value of 1.2×10^{10} L mol^{-1} s^{-1} for the reaction of e_{aq}^- with $ONOO^-$, we derived the predicted curve shown in Figure 7. This derived rate constant is similar to those for the reactions of e_{aq}^- with NO, NO_2, or NO_2^-.[30]

Discussion

Although several mechanisms may be suggested for the formation of peroxynitrite after the reaction of $^{\bullet}NH_2$ with O_2,

SCHEME 1: Proposed Mechanism for the Formation of NO from the Reaction of $^{\bullet}NH_2$ with O_2; Possible Deprotonation of Intermediates Is Ignored

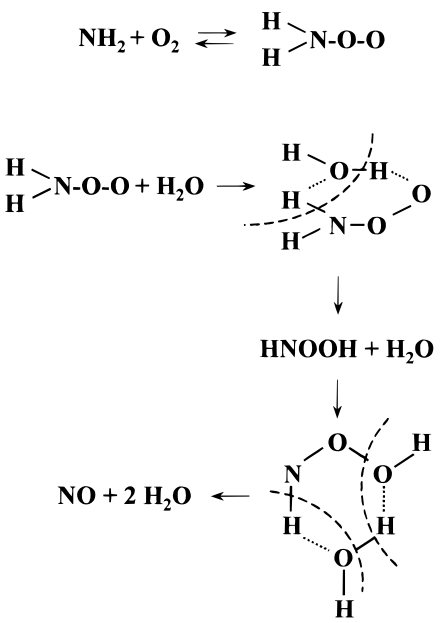

the results are consistent with a mechanism in which an intermediate peroxyl radical, $NH_2O_2^{\bullet}$, is formed,

$$H_2N{-}O{-}O^{\bullet} \rightarrow H{-}N{-}O{-}O{-}H \rightarrow NO + H_2O \quad (11)$$

which then decomposes to a nonabsorbing species which subsequently reacts with $O_2^{\bullet-}$. The most likely candidate for the reaction that finally results in peroxynitrite is the known fast reaction of $O_2^{\bullet-}$ with NO ($k = 6.7 \times 10^9$ L mol^{-1} s^{-1})[13]

$$NO + O_2^{\bullet-} \rightarrow ONOO^- \quad (10)$$

It is clear that the reaction of $^{\bullet}NH_2$ and O_2 does not take place in the gas phase, so how is this reaction feasible in the aqueous phase? Theoretical considerations have indicated that the peroxyl intermediate proposed is not strongly bound. Benson estimated the bond strength for $NH_2{-}O_2$ to be 16 ± 16 kJ mol^{-1}.[31] A subsequent calculation by Melius and Binkley indicated that the peroxyl radical, $NH_2O_2^{\bullet}$, is about 20 kJ mol^{-1} more stable than the separated reactants.[32] These calculations also place the rearrangement product HNOOH at about 5 kJ mol^{-1} higher energy than $NH_2O_2^{\bullet}$. The cyclic transition state which lies between these two isomers was calculated to be 170 kJ mol^{-1}.[32] A subsequent calculation based on the estimated strain in the four-membered ring suggested a barrier of 126 kJ mol^{-1}.[33] In either case, neither stabilization of the peroxyl radical nor reaction over this barrier is expected to be important in the gas phase at room temperature. Theory, then, is in agreement with the lack of reactivity of $^{\bullet}NH_2$ toward O_2 observed in the gas phase. In aqueous solutions, however, there is an alternate mechanism possible. The conversion of $NH_2O_2^{\bullet}$ to HNOOH can be catalyzed by a water molecule, or by a NH_3 molecule or an OH^- anion, via a transition state with a six-membered ring (see Scheme 1). The final step in the scheme, the decomposition of HNOOH to H_2O + NO, is a highly exothermic process, with $\Delta H = -320$ kJ mol^{-1}.[33]

The proposed mechanism for the reaction of $^{\bullet}NH_2$ with O_2 is in basic accord with our observations, those made previously on this system, and the calculated potential energy surface. These details have been obscured in the past due to the very weak absorption exhibited by the aminyl radical. The initial decay of the $^{\bullet}NH_2$ absorption is rapid, and indeed, the rate constant we derive is the same as the rate constant reported by Pagsberg.[4] In our case, increased sensitivity allowed us to see that the decay rate slowed, due to the reverse reaction, and therefore represents a lower limit. The reversibility of the reaction is in accord with the theoretical calculations and with the lack of an overall reaction in the gas phase. The fact that we can observe the intermediate $^{\bullet}NH_2O_2$ may also reflect some stabilization of this species due to strong hydrogen bonding in water. The rearrangement of the $^{\bullet}NH_2O_2$ in water is supported by the observation that there appears to be some base catalysis of this process. The subsequent decomposition of the rearranged product to NO and H_2O is in accord with the known decomposition of NO_2^{2-} to NO and H_2O.[34,35]

In this work, we confirmed that the spectrum of the final product from the γ-radiolysis of oxygenated ammonia solutions is identical to that of peroxynitrite and that the yield is identical to the initial yields of the hydroxyl radical and the electron (with some easily explained loss at long times). In the flash photolysis experiments, the yield of peroxynitrite was very low, however. This strongly supports the role of $^{\bullet}O_2^-$ in the formation of peroxynitrite, since this would only be formed to a minor degree in the flash photolysis experiments, whereas it would be formed quantitatively in the γ-radiolysis studies.

Although we can explain the basic chemistry taking place during the oxidation of ammonia, we have been unable to derive quantitative rate constants for the important steps: the reaction of $^{\bullet}NH_2$ with O_2 and its reverse and the decomposition of $NH_2O_2^{\bullet}$ into final products. A rate constant for the initial step of about 10^9 L mol^{-1} s^{-1} is consistent with all the results, however. This suggested mechanism also can explain our observations with ZnTSPP as a competing reactant. We have modeled this system and find that, if we assume that $NH_2O_2^{\bullet}$ oxidizes ZnTSPP, but much more slowly than does $^{\bullet}NH_2$, we can explain the curvature in Figure 1.

References and Notes

(1) Atkinson, R.; Baulch, D. L.; Cox, R. A.; Hampson, R. F.; Kerr, J. A.; Troe, J. *J. Phys. Chem. Ref. Data* **1992**, *21*, 1125.
(2) Hickel, B.; Shested, K. *Radiat. Phys. Chem.* **1992**, *39*, 355.
(3) Tyndall, G. S.; Orlando, J. J.; Nickerson, K. E.; Cantrell, C. A.; Calvert, J. G. *J. Geophys. Res.* **1991**, *96*, 20761.
(4) Pagsberg, P. B. Investigation of the NH_2 radical produced by pulse radiolysis of ammonia in aqueous solution. RISØ Report, 1972.
(5) Men'kin, V. B.; Makarov, I. E.; Pikaev, A. K. *High Energy Chem.* **1991**, *25*, 48.
(6) Neta, P.; Maruthamuthu, P.; Carton, P. M.; Fessenden, R. W. *J. Phys. Chem.* **1978**, *82*, 1875.
(7) Ershov, B. G.; Mikhailova, T. L.; Gordeev, A. V.; Spitsyn, V. I. *Dokl. Phys. Chem.* **1988**, *300*, 506.
(8) Giguere, P. A.; Herman, K. *Chem. Phys. Lett.* **1976**, *44*, 273.
(9) Mikhailova, T. L.; Ershov, B. G. *Russ. Chem. Bull.* **1993**, *42*, 235.
(10) Rigg, T.; Scholes, G.; Weiss, J. *J. Chem. Soc.* **1952**, 3034.
(11) Schönherr, S.; Röhl, K.; Schrader, R. *Z. Anorg. Allg. Chem.* **1980**, *465*, 225.
(12) Huie, R. E. Free radical chemistry of the atmospheric aqueous phase. In *Current Problems and Progress in Atmospheric Chemistry*; Barker, J. R., Ed.; World Scientific Publishing Co.: Singapore, 1995; Vol. 3, p 374.
(13) Huie, R. E.; Padmaja, S. *Free Radical Res. Commun.* **1993**, *18*, 195.
(14) The identification of commercial equipment of materials does not imply recognition or endorsement by the National Institute of Standards and Technology, nor does it imply that the material or equipment identified are necessarily the best available for the purpose.
(15) Laszlo, B.; Kurylo, M. J.; Huie, R. E. *J. Phys. Chem.* **1995**, *99*, 11701.
(16) Laszlo, B.; Huie, R. E.; Kurylo, M. J.; Miziolek, A. W. *J. Geophys. Res.* **1997**, *102*, 1523.
(17) Neta, P.; Huie, R. E. *J. Phys. Chem.* **1985**, *89*, 1783.
(18) *CRC Handbook of Chemistry and Physics*; Weast, R. C., Astle, M. J., Eds.; CRC Press: Boca Raton, FL, 1979.

(19) Herrmann, H.; Reese, A.; Zellner, R. *J. Mol. Struct.* **1995**, *348*, 183.
(20) Bao, Z.-C.; Barker, J. R. *J. Phys. Chem.* **1996**, *100*, 9780.
(21) Buxton, G. V.; McGowan, S.; Salmon, G. A.; Williams, J. E.; Wood, N. D. *Atmos. Environ.* **1996**, *14*, 2483.
(22) McElroy, W. J. *J. Phys. Chem.* **1990**, *94*, 2435.
(23) Jiang, P. Y.; Katsumura, Y.; Nagaishi, R.; Domae, M.; Ishikawa, K.; Ishigure, K.; Yoshida, Y. *J. Chem. Soc., Faraday Trans.* **1992**, *88*, 1653.
(24) Dressler, K.; Ramsay, D. A. *Philos. Trans. R. Soc.* **1959**, *251A*, 553.
(25) Neta, P.; Huie, R. E. *J. Phys. Chem.* **1986**, *90*, 4644.
(26) Men'kin, V. B.; Makarov, I. E.; Pikaev, A. K. *High Energy Chem.* **1988**, *22*, 333.
(27) Hughes, M. N.; Nicklin, H. G. *J. Chem. Soc. A* **1968**, 450.
(28) Neta, P.; Harriman, A. *J. Chem. Soc., Faraday Trans. 2* **1985**, *81*, 123.
(29) Løgager, T.; Shested, K. *J. Phys. Chem.* **1993**, *97*, 6664.
(30) Ross, A. B.; Mallard, W. G.; Hellman, W. P.; Buxton, G. B.; Huie, R. E.; Neta, P. *NIST Stand. Ref. Database* **1994**, *40*.
(31) Benson, S. W. Comment. *18th Symp. (Int.) Comb. Proc*. **1982**.
(32) Melius, C. F.; Binkley, J. S. Reactions of NH and NH_2 with O and O_2. In *The Chemistry of Combustion Processes*; American Chemical Society: Washington, DC, 1984; Vol. 249, p 103.
(33) Bozzelli, J. W.; Dean, A. M. *J. Phys. Chem.* **1989**, *93*, 1058.
(34) Graetzel, M.; Henglein, A.; Lilie, J.; Beck, G. *Ber. Bunsen-Ges. Phys. Chem.* **1969**, *73*, 3.
(35) Broszkiewicz, R. K. *Bull. Acad. Pol. Sci., Ser. Sci. Chim.* **1976**, *24*, 221.